Atmos. Chem. Phys. Discuss., 8, 17297–17341, 2008
www.atmos-chem-phys-discuss.net/8/17297/2008/

Atmospheric Chemistry and Physics Discussions

This discussion paper is/has been under review for the journal *Atmospheric Chemistry and Physics (ACP)*. Please refer to the corresponding final paper in *ACP* if available.

Investigation of NO_x emissions and NO_x-related chemistry in East Asia using CMAQ-predicted and GOME-derived NO_2 columns

K. M. Han[1], C. H. Song[1], H. J. Ahn[1], C. K. Lee[1,2], A. Richter[3], J. P. Burrows[3], J. Y. Kim[4], J. H. Woo[5], and J. H. Hong[6]

[1]Department of Environmental Science and Engineering, Gwangju Institute of Science and Technology (GIST), Gwangju, Korea
[2]Dept. of Physics and Atmospheric Science, Dalhousie Univ., Halifax, Nova Scotia, Canada
[3]Institute of Environmental Physics, University of Bremen, Otto-Hahn-Allee 1, 28359 Bremen, Germany

[4]Hazardous Substance Research Center, Korea Institute of Science and Technology (KIST), Seoul, Korea
[5]Dept. of Advanced Technology Fusion, Konkuk University, Seoul, Korea
[6]Air Pollution Cap System Division, National Institute of Environmental Research (NIER), Incheon, Korea

Received: 21 July 2008 – Accepted: 4 August 2008 – Published: 17 September 2008

Correspondenco to: C. H. Song (chsong@gist.ac.kr)

Abstract

This study examined the estimation accuracy of NO_x emissions over East Asia with particular focus on North China and South Korea due to their strong source (North China)-receptor (South Korea) relationship. In order to determine contributions of North China emissions to South Korean air quality accurately, it is important to examine the accuracy of the emission inventories of both regions. In this study, NO_2 columns from the US EPA Models-3/CMAQ model simulations carried out using the 2001 ACE-ASIA (Asia Pacific Regional Aerosol Characterization Experiment) emission inventory over East Asia were compared with the GOME-derived NO_2 columns. There were large discrepancies between the CMAQ-predicted and GOME-derived NO_2 columns in the fall and winter seasons. In particular, while the CMAQ-predicted NO_2 columns produced larger values than the GOME-derived NO_2 columns over South Korea (receptor region) for all four seasons, the CMAQ-predicted NO_2 columns produced smaller values than the GOME-derived NO_2 columns over North China (source region) for all seasons with the exception of summer. It is believed that there might be some estimation error in the NO_x emissions as well as large uncertainty in NO_x loss rates over North China and South Korea. Regarding the latter, this study further focused on the biogenic VOC emissions that were strongly coupled with NO_x chemistry in East Asia. It was found that the rates of NO_x loss determined by CMAQ modeling studies might be significantly low due to the possible overestimation of biogenic isoprene emissions during summer, particularly in China. In addition, due to the possible overestimation of isoprene emissions, the CMAQ-modeled NO_2/NO_x ratios might show an incorrectly high level, compared with the actual NO_2/NO_x ratios. In addition to the retarded NO_x chemical loss rates and overestimated NO_2/NO_x ratios, the omission of soil NO_x emissions over North China during summer can lead to an underestimation of NO_x emissions over North China during summer. Overall, it is estimated that the NO_x emissions in North China are underestimated possibly by ~50% over an entire year. In order to confirm the uncertainty in NO_x emissions, the NO_x emission over South Korea was fur-

ACPD

8, 17297–17341, 2008

ther investigated using the ACE-ASIA inventory, REAS (Regional Emission inventory in ASia) and CAPSS (Clean Air Policy Support System) by NIER (National Institute of Environmental Research) in Korea. The NO_x emissions from ACE-ASIA and the REAS inventories appear to be approximately 2 times larger for mega-cities in Korea than that from the CAPSS inventory. In contrast, the NO_x emissions of ACE-ASIA and REAS inventories are only 10% smaller for North China than the recently-estimated "date-back" ANL (Argonne National Laboratory) inventory. A comparison between the CMAQ-predicted and GOME-derived NO_2 columns indicated that both the ACE-ASIA and REAS inventories have some uncertainty in NO_x emissions over North China (A) and South Korea (C), which can lead to some error in modeling the formation of ozone and secondary aerosols in South Korea and North China.

1 Introduction

Nitrogen oxides ($NO_x \equiv NO+NO_2$) emitted from anthropogenic sources, such as fossil fuel combustion and biomass burning, as well as natural sources, such as lightning and microbiological processes in soil, play important roles in tropospheric ozone chemistry and secondary aerosol formation. Several studies have focused on NO_x emissions from China to determine their influence on air quality and aerosol radiative forcing in East Asia (e.g. Uno et al., 2007; Wang et al., 2007; Zhang et al., 2007). Recent studies using satellite measurements reported that NO_2 columns (or NO_2 vertical column density, VCD) have increased significantly in Central East Asia since 2001 (Richter et al., 2005; van der A et al., 2006; He et al., 2007). Such increases in NO_x emissions over China were confirmed partly by a bottom-up emission inventory study (Zhang et al., 2007). In order to test the accuracy of NO_x emissions, several studies were carried out over East Asia comparing the 3-D model-predicted NO_2 columns with satellite-derived NO_2 columns (Kunhikrishnan et al., 2004; Ma et al., 2006; Uno et al., 2007). The comparisons revealed large inconsistencies between the NO_2 columns from the 3-D CTM (Chemical Transport Model) simulations and the satellite-derived NO_2 columns.

For example, Uno et al. (2007) reported that the 3-D CTM-derived NO_2 columns with the REAS (Regional Emission inventory in ASia) emission inventory were lower by a factor of 2–4 over polluted Central East China, compared with the GOME (Global Ozone Monitoring Experiment)-retrieved NO_2 columns. In addition, Ma et al. (2006) also reported that the 3-D CTM-derived NO_2 columns with the ACE-ASIA (Asia Pacific Regional Aerosol Characterization Experiment) emission inventory underestimated the NO_x emissions over China during the summer for the year 2000 by more than 50% compared with the GOME-derived NO_2 columns. However, there has been no detailed investigation carried out as to how and why the NO_2 columns over China were under-predicted by 3-D CTM simulation using the ACE-ASIA or REAS inventory. In addition, there are no reports on the possibly important relationship between the rates of NO_x loss and biogenic isoprene emissions in East Asia, even though it could be an important factor for evaluating NO_x emissions. Biogenic emissions are important because they can control the levels of OH radicals, which can affect the NO_x chemical loss rates.

On the other hand, an accurate estimation of NO_x emissions in China is important because NO_x emissions from North China tend to persistently affect the air quality of South Korea (e.g. Arndt et al., 1998). From 2003, the Korean government began to implement an ambitious pollution abatement policy aimed at improving the air quality of Seoul Metropolitan area, called the "Total Air Pollution Load Management System", by reducing the levels of secondary pollutants, such as O_3, PANs (Peroxy Acetyl Nitrates), and nitrate (Korean Ministry of Environment, 2006). This policy included a specific plan to reduce the total NO_x emissions from the Seoul Metropolitan area by 53%, from 309 387 Ton yr^{-1} (2001) to 145 412 Ton yr^{-1} (2014). The reference and target years for the Total Air Pollution Load Management System are 2001 and 2014, respectively. However, the critical and largest uncertainty in implementing this policy is to evaluate and quantify accurately the influences of the emissions outside the policy domain on the air quality of the Seoul Metropolitan area. Due to the strong and persistent source-receptor relationship between North China and South Korea, it is important to use accurate emission inventories for both the source ("North China") and the receptor

regions ("Seoul Metropolitan area" or "South Korea") for the reference and target years, 2001 and 2014.

This study examined the accuracy of NO_x emissions from North China and South Korea using the CMAQ-simulated and GOME-derived NO_2 columns. In addition to the uncertainty in NO_x emission itself, this paper also discussed the possibly important uncertainty factors that could cause inconsistencies between the CMAQ-derived and GOME-derived NO_2 columns. Particularly, the HO_x-NO_x-isoprene photochemistry in East Asia was examined in detail on account of its strong relationship with the inconsistency between the CMAQ-simulated and GOME-derived NO_2 columns in East Asia.

2 Experimental methods

In this study, a three-dimensional Eulerian CTM simulation over East Asia was carried out in conjunction with the Meteorological fields generated from the PSU/NCAR MM5 (Pennsylvania state University/National Center for Atmospheric Research Meso-scale Model 5) model in order to compare the CTM-predicted NO_2 columns with the satellite (GOME)-derived NO_2 columns.

2.1 US EPA models-3/CMAQ modeling

In this study, a 3-D Eulerian CTM, US EPA Models-3/CMAQ (Community Multi-scale Air Quality) model was used in conjunction with the MET fields generated from PSU/NCAR MM5 modeling over an approximately 3 week period for four seasons: Late Fall (9 November 2001–27 November 2001), Spring (25 March 2002–13 April 2002), Late Summer (24 August 2002–13 September 2002), and Winter (11 February 2003–28 February 2003) (Byun and Ching, 1999; Byun and Schere, 2006). The details of the modeling conditions were reported by Song et al. (2008). For the MET fields, the $2.5^{\circ} \times 2.5^{\circ}$ resolved re-analyzed National Centers for Environmental Prediction (NCEP)

data with automated data processing (ADP) of the global surface and upper air observations were employed using four-dimensional data assimilation (FDDA) techniques (Stauffer and Seaman, 1990, 1994). The MET fields were generated at "1 h intervals" during the four episode periods. The CMAQ modeling system then used the meteorological fields generated from the PSU/NCAR MM5 and emission fields. The schemes selected in CMAQ modeling are as follows: the piece-wise parabolic method (PPM) for advection (Collela and Woodward, 1984); 4th generation carbon bond mechanism (CBM 4) for gas phase chemistry (Gery et al., 1989); the Carnegie-Mellon University (CMU) aqueous chemistry mechanism for cloud chemistry (Pandis and Seinfeld, 1989; Fahey and Pandis, 2003); the AERO3 module for particulate dynamics and aerosol thermodynamics (Binkowski and Roselle, 2003); and the Wesley scheme for the dry deposition of both gaseous and particulate species (Wesley, 1989). The 4th generation carbon bond mechanism for gas-phase chemistry included explicit VOC species, such as ALD2 (higher aldehyde, C>2), ETH (ethane), FORM (formaldehyde), ISOP (isoprene), OLE (olefin), PAR (paraffin), TOL (toluene), and XYL (xylene). As indicated above, far more detailed atmospheric chemistry and physical processes, aerosol dynamics, and thermodynamic gas-aerosol processes were considered in these calculations than in other global and regional chemistry-transport modeling studies in order to better consider the atmospheric fate of NO_x. For example, in this study the analysis was not restricted to "clear sky conditions". In other words, it fully considered cloud chemistry, wet scavenging, and the effects of clouds on the photolysis reaction rates.

The horizontal domain of CMAQ modeling reported in Fig. 1 covered the region from approximately 100° E to 150° E and 20° N to 50° N, which included Korea, Japan, China, and parts of Mongolia and Russia with a 108 km×108 km grid resolution. For vertical resolution, 24 layers were used with σ-coordinates using the model-top at 180 hPa. For comparison, NO_2 vertical column loading was integrated from the surface to 250 hPa (approximately corresponding to ~10 km a.s.l. in these calculations). The CMAQ-modeled NO_2 columns were averaged between 10:00 LST and 12:00 LST because the GOME measurements were taken approximately at 10:30 LST over East

Asia. The total number of the grid points in the CMAQ model calculation was 36 432. Figure 1 also shows the four main study regions used for the comparison studies: i) North China (Region A, 30° N–42° N; 110° E–125° E); ii) South China (Region B, 22° N–30° N; 108° E–122° E); iii) South Korea (Region C, 33.5° N–40° N; 125° E to 130° E); and iv) Japan (Region D, 31° N–40° N; 130° E–142° E). Here, the remote continental areas in China were excluded from our analysis, partly because they are remote areas, and the NO_2 columns showed a similar order of magnitude of the absolute errors to the GOME measurements ($\sim 10^{15}$ molecules cm^{-2}).

2.2 Emissions

Emission is an important input parameter in a modeling study. Poor agreement between 3-D modeling studies and satellite measurements is expected if the emission inventories incorrectly reflect the seasonal and spatial emission flux from the various sources. In order to consider anthropogenic emissions, 1°×1° resolved emission data for 9 major species, including SO_2, NO_x, CO, NMVOCs (Non-Methane Volatile Organic Compounds), CH_4, NH_3, CO_2, BC, and OC, were obtained from the official ACE-ASIA and TRACE-P (Transport and Chemical Evaluation over Pacific) emission web site at the University of Iowa (http://www.cgrer.uiowa.edu/EMISSION_DATA/index.htm). Streets et al. (2003) provided detailed information on the emission inventory (hereafter, labeled the ACE-ASIA inventory) used in this study. The ACE-ASIA emission inventory included NO_x emissions from fossil fuels and biofuel combustion as well as biomass (vegetation) burning in East Asia. However, the inventory did not consider the NO_x emissions from lightning and microbial activity in soil. In general, emission from lightning is believed to make a small contribution to the total NO_x budget (Martin et al., 2003). On the other hand, Wang et al. (2007) reported that soil NO_x emissions might be important, accounting for up to ~43% of the combustion source during summer in East Asia. In addition, the original ACE-ASIA emission inventory was built up for the year 2000. Therefore, the NO_x emissions for East Asia were modified slightly by multiplying a factor of 1.05 in order to account for an annual increase in NO_x emissions from

China for the year 2001 (Zhang et al., 2007).

Anthropogenic NMVOC emissions were assumed to be constant without any seasonal variation. In this study, chemical speciation (chemical species splitting) of the total NMVOC emissions in East Asia was performed using the SPECIATE database built up by the US EPA. The major biogenic $1^{\circ}\times1^{\circ}$ resolved emissions data of isoprene and monoterpene were obtained from the Global Emissions Inventory Activity (GEIA, http://www.geiacenter.org/), which was created as an activity of the International Geosphere-Biosphere Program (IGBP).

2.3 NO_2 retrieval algorithm from ESA/ERS-2 GOME platform

GOME was launched on the ERS-2 satellite by European Space Agency (ESA) in April 1995. It is a nadir-scanning double-monochromator, and obtains approximately 30 000 radiance spectra each day covering the ultraviolet and visible wavelengths from 240 to 790 nm at a moderate spectral resolution of 0.17 to 0.33 nm. Because GOME is a nadir viewing instrument, both tropospheric and stratospheric absorptions contribute to the measured signals. The ground scene of GOME typically has a footprint of $320\times40\,km^2$. Total ground coverage is obtained within 3 days at the equator with a 960 km wide track swath (4.5 s forward scan and 1.5 s backward scan).

The NO_2 analysis for GOME is based on a Differential Optical Absorption Spectroscopy (DOAS) retrieval method (Richter and Burrows, 2002; Richter et al., 2005). The wavelength range of 425–450 nm was used for the NO_2 DOAS fit because the differential absorption is large and interference by other species is small. In addition to the NO_2 cross-section (Burrows et al., 1998), the cross-sections of O_3 (Burrows et al., 1999), O_4 (Greenblatt et al., 1990), H_2O (Rothman et al., 1992), a synthetic Ring spectrum (Vountas et al., 1998), and an undersampling correction (Chance, 1998) were included in the fit. In order to calculate the tropospheric NO_2 slant column, the stratospheric contribution of NO_2 to the measured slant column was removed by subtracting the slant column taken on the same day at the same latitude in the 180°–230° longitude region from the total slant column using the reference sector method (Richter and

Burrows, 2002). Cloud screening was applied to remove measurements with a cloud fraction >0.3, as determined from the GOME measurements using the FRESCO (Fast Retrieval Scheme for Clouds from the Oxygen A-band) algorithm (Koelemeijer et al., 2001). The tropospheric slant column was then converted to a vertical tropospheric column using the appropriate air mass factor (AMF). The AMF is defined as the ratio of the observed slant column to the vertical column and was calculated with using the radiative transfer model (SCIATRAN) (Rozanov et al., 1997). The monthly averaged AMF on a 2.5°×2.5° grid was determined using the NO_2 vertical profiles (shape facor) from a global chemical transport model, MOZART-2 (Model for Ozone and Related Tracers).

The error budget of satellite measurements of tropospheric NO_2 columns from GOME has been discussed in detail (e.g. Richter and Burrows, 2002; Martin et al., 2003; Boersma et al., 2004; Richter et al., 2005). The main contributions to the error are random fitting uncertainties, uncertainties related to the subtraction of the stratospheric contributions, uncertainties from residual clouds, and AMF. The total uncertainties in the retrieval of tropospheric NO_2 columns over continental source regions is largely determined by the AMF calculation due to surface reflectivity, clouds, aerosols, and the trace gas profile. An overall assessment of errors leads to 5×10^{14}–1×10^{15} molecules cm^{-2} for monthly averages over polluted areas (Richter and Burrows, 2002; Richter et al., 2005).

3 Results and discussions

In order to properly determine the contributions from North China emissions to air quality of South Korea, it is important to evaluate the accuracy of the NO_x emission inventories over both regions and understand NO_x-related gas-phase chemistry. Initially, 3-day backward trajectory analysis was conducted (Sect. 3.1) to confirm the strong source-receptor relationship between North China (A) and South Korea (C). Subsequently, the CMAQ-predicted NO_2 columns are then spatially and seasonally compared with the GOME-derived NO_2 columns (Sect. 3.2). The ACE-ASIA NO_x emissions in North

China (A, source region) and South Korea (C, receptor region) are then compared with other recently-released inventories such as, REAS, "date-back" ANL (Argonne National Laboratory) inventory, and CAPSS (Sect. 3.3).

3.1 Backward trajectory analysis

In this study, a 3-day backward trajectory analysis for each month of 2001 was carried out using the NOAA HYSPLIT model (Draxler, 1999) to confirm the persistent source (North China, A)-receptor (South Korea, C) relationship, as well as to determine how frequently the air masses travel from North China (A) to South Korea (C). Approximately 20 days per month were selected. The trajectory ends at a point (37.5° N, 127.0° E) at an altitude of 1 km under which Seoul is located. As shown in Fig. 2, the air masses traveled from North China (A) to South Korea (C) during almost the entire year. However, in July, the air masses appear to be affected by the emissions from South China (B). In August and September, the air masses arrive in Seoul from the North, East, South (August) and the Northeast (September). Although air masses do not always travel from North China (A) to Seoul during July, August, and September, it is clear that the South Korean air quality is most strongly and persistently affected by the emissions from North China (A) throughout almost the entire year. Therefore, in the framework of the source-receptor relationship, this study focused particularly on the emissions from two regions, North China (A) and South Korea (C).

3.2 CMAQ-predicted and GOME-derived NO_2 columns and NO_x-related chemistry in East Asia

3.2.1 CMAQ-predicted vs. GOME-derived NO_2 columns

Figure 3 shows the spatial distributions of the CMAQ-predicted NO_2 columns and the GOME-derived NO_2 columns for four episodes over East Asia. Figure 4 shows a close-up of the area of South Korea for better visualization. There were large discrepancies

ACPD
8, 17297–17341, 2008

between the two quantities in the late fall and winter seasons (i.e. cold seasons), as well as strong seasonal variations, particularly in the GOME-derived NO_2 columns. Interestingly, the CMAQ-predicted NO_2 columns were larger than the GOME-derived NO_2 columns for all seasons over South Korea (C) (Fig. 4). On the other hand, the CMAQ-predicted NO_2 columns over North China (A) were smaller than the GOME-derived NO_2 columns for all seasons except for summer (Fig. 3). Note that the differences between the CMAQ-predicted and the GOME-derived NO_2 columns in the third column in Figs. 3 and 4 have negative values ("blue colors") over North China (A) and positive values ("red-orange colors") over South Korea (C). Scatter plots between the CMAQ-predicted and GOME-derived NO_2 columns were also made for North China (A), South China (B), South Korea (C), and Japan (D) for further confirmation. Figure 5 shows that there are no clear seasonal trends in South China (B) and Japan (D), whereas the CMAQ-predicted NO_2 columns over South Korea (C) are obviously larger than the GOME-derived NO_2 columns for all seasons. In addition, the CMAQ-predicted NO_2 columns over North China (A) were clearly smaller than the GOME-derived NO_2 columns for all seasons except for summer. These results are further confirmed through statistical analyses (see Sect. 3.2.2). These results suggest that there are some errors in the estimations of NO_x emissions over North China (A) and South Korea (C) in the ACE-ASIA NO_x emission inventory. Of course, this inference should be valid only when the following assumption is held: In CMAQ modeling, emission is the largest uncertainty, and the other atmospheric chemical and physical processes are reasonably accurate. In this study, we chose the GOME-derived NO_2 columns as reference values, although the GOME measurements also have uncertainties, mainly from the assumptions made in the radiative transfer calculations (Richter et al., 2005). In this study, we focused on the highly polluted East Asian regions where the monthly averages of NO_2 columns reach $\sim 2\times10^{16}$ molecules cm^{-2} (see Figs. 3, 4, and 5; also refer to Uno et al., 2007). The NO_2 columns are larger than the magnitudes of overall errors of the GOME NO_2 column measurements, 5×10^{14}–1×10^{15} molecules cm^{-2}. An attempt was also made to determine why the difference between the CMAQ-predicted

and GOME-derived NO_2 columns became minimal only during summer in Fig. 3. This issue is discussed in detail in Sect. 3.2.3.

3.2.2 Statistical analysis

Table 1 shows the seasonal and regional statistical analyses between the CMAQ-predicted and GOME-derived NO_2 columns. The following four statistical parameters were introduced for statistical analyses: i) Root Mean Square Error (RMSE, absolute error); ii) Mean Normalized Gross Error (MNGE, relative error); iii) Mean Bias (MB, absolute bias); and iv) Mean Normalized Bias (MNB, relative bias). The four statistical parameters are defined in Eqs. (1) to (4):

$$\mathrm{RMSE} = \sqrt{\frac{1}{N}\sum_{1}^{N}\left(\mathrm{NO}_{2,\mathrm{CMAQ}} - \mathrm{NO}_{2,\mathrm{GOME}}\right)^2} \quad (1)$$

$$\mathrm{MNGE} = \frac{1}{N}\sum_{1}^{N}\left(\frac{\left|\mathrm{NO}_{2,\mathrm{CMAQ}} - \mathrm{NO}_{2,\mathrm{GOME}}\right|}{\mathrm{NO}_{2,\mathrm{GOME}}}\right) \times 100 \quad (2)$$

$$\mathrm{MB} = \frac{1}{N}\sum_{1}^{N}\left(\mathrm{NO}_{2,\mathrm{CMAQ}} - \mathrm{NO}_{2,\mathrm{GOME}}\right) \quad (3)$$

$$\mathrm{MNB} = \frac{1}{N}\sum_{1}^{N}\left(\frac{\mathrm{NO}_{2,\mathrm{CMAQ}} - \mathrm{NO}_{2,\mathrm{GOME}}}{\mathrm{NO}_{2,\mathrm{GOME}}}\right) \times 100 \quad (4)$$

In Table 1, RMSE analysis showed that the magnitudes of the "absolute" differences were much larger over North China (A) and South Korea (C) than over South China (B) and Japan (D) (These are denoted as "bold fonts" in Table 1). Large uncertainties are expected over North (A) and South Korea (C). The MNGEs range from 39.6% to 59.0% over North China (A) and from 54.5% to 121.2% over South Korea (C). Relative bias

analysis (MNB) showed that the CMAQ-predicted NO_2 columns tends to have positive biases ranging from 41.1% to 117.6% compared with the GOME-derived NO_2 columns over South Korea (C). In contrast, over North China (A), the CMAQ-predicted NO_2 columns tend to have low biases ranging from −8.6% to −56.9% with the exception of summer. These statistical analyses are also in line with the results reported in Sect. 3.2.1.

3.2.3 Summer anomaly due to possible overestimation of isoprene emissions in East Asia

The first and second columns in Fig. 3 show seasonal variations of the NO_2 columns over East Asia. The CMAQ-derived NO_2 columns show weak seasonal variations in North China (Region A), whereas the GOME-derived NO_2 columns show strong seasonal variations. The differences between the two NO_2 columns reduce to almost zero during summer, and are also small over North China (A) during spring (Fig. 3). Table 1 shows that the MNB has a positive value over North China (A) only during summer. There are two factors that may be involved in these phenomena: i) seasonal variations in NO_x emissions; and ii) seasonal variations in the NO_x chemical loss rates. First, the distribution of NO_2 columns can be influenced by the seasonal variations in NO_x emissions. However, Streets et al. (2003) reported almost no seasonal variations in anthropogenic NO_x and SO_2 emissions, which is in contrast to black carbon (BC) emissions. The monthly fraction of the NO_x emissions is almost constant, as shown in Fig. 6, even though the fractions of NO_x emissions increase slightly in December and January. Therefore, the seasonal changes in NO_x emissions are not a likely cause of the seasonal variations in the NO_2 columns (Note that uniform NO_x emission fluxes were also assumed in the CMAQ model based on the almost constant NO_x emissions shown in Fig. 6). Secondly, in order to explain this anomalous (or unexpected) phenomenon in NO_2 concentration, this study examined the seasonal variations in NO_x chemical loss rates in East Asia. The chemical mechanisms for NO_x loss are HNO_3 and nitrate formation (i.e. N(V) formation) in the atmosphere. Both nitric acid and par-

ticulate nitrate form from NO_x by Reactions (R1) through to (R5) as follows:

$$NO_2 + OH + M \rightarrow HNO_3 \quad (M: \text{ third body}) \tag{R1}$$

$$NO_3 + HCHO \rightarrow HNO_3 + CHO \tag{R2}$$

$$NO_3 + CH_3CHO + O_2 \rightarrow HNO_3 + CH_3CO_3 \tag{R3}$$

$$NO_3 \xrightarrow{\text{Hetro.}} NO_3^- \tag{R4}$$

$$N_2O_5 + H_2O \xrightarrow{\text{Hetro.}} 2H^+ + 2NO_3^- \tag{R5}$$

Therefore, the NO_x chemical loss rate (L_{NO_x}) can be constructed by Eq. (5):

$$L_{NO_x} \equiv k_1 [NO_2][OH] + k_2 [NO_3] [HCHO] + k_3 [NO_3] [ALD2] + k_{4,h} [NO_3] + 2k_{5,h}[N_2O_5] \tag{5}$$

where, the first, second and third terms in the right hand side of Eq. (5) represent the NO_x chemical loss rate due to HNO_3 formation via Reactions (R1), (R2), and (R3), respectively. The fourth and fifth terms represent heterogeneous nitrate formation by Reactions (R4) and (R5), respectively. In Eq. (5), the heterogeneous mass transfer coefficients (s^{-1}) of $k_{4,h}$ and $k_{5,h}$ for NO_3 and N_2O_5 radicals were calculated using the Schwartz formula ($k_i = \gamma_i S_i v_i/4$) (Schwartz, 1986). In the Schwartz formula, γ_i, S_i, and v_i represent the reaction probability, aerosol surface density ($\mu m^2\, cm^{-3}$), and molecular mean velocity ($cm\, s^{-1}$) for species i, respectively. Among the five pathways for removing NO_x , L_{NOx} is dominated by Reaction (R1), i.e. the first term in Eq. (5). The third column in Fig. 7 shows the model-predicted, spatial distributions of the NO_x chemical loss rates at the surface. As expected, the rates of NO_x loss are much faster during spring and summer than during fall and winter. In addition, the NO_x chemical loss rates are rapid, particularly around metro-city areas, such as Beijing, Shanghai, Taipei, Seoul, Busan, and Tokyo, where OH concentrations are relatively high. However, Fig. 7

ACPD
8, 17297–17341, 2008

shows an unexpected phenomenon. The L_{NO_x} in spring is, on average, larger than that in summer, particularly over Regions A, B, and C (the three regions are indicated by the three white boxes in Fig. 7). It is possible that this is caused by biogenic VOC emissions in summer (the anthropogenic NMVOC emissions were kept constant in the CMAQ modeling of the four episodes). The first column in Fig. 7 shows the biogenic isoprene concentrations at the surface for the four episodes. The isoprene concentrations were highest during summer. Biogenic isoprene emissions influence the formation of ozone, and affect rates of NO_x removal by controlling the levels of hydroxyl radicals. Hydroxyl radicals (OH) are produced by $O^{1D}+H_2O$ Reaction (R6) and HONO photo-dissociation (R7). Hydroxyl radicals (OH) are converted to perhydroxyl radicals (HO_2) or organic peroxyl radicals (RO_2) through Reactions (R8), (R9), and (R10) (in the Reaction R10, RH indicates non-methane hydrocarbons). Formaldehydes (HCHO) are also an important source of hydroxyl radicals in that perhydroxyl radicals (HO_2) are produced by HCHO photo-dissociation (R11) and a HCHO+OH Reaction (R12).

$$O^{1D} + H_2O \rightarrow 2OH \quad \text{(R6)}$$

$$HONO + h\nu \rightarrow NO + OH \quad \text{(R7)}$$

$$OH + CO + O_2 \rightarrow CO_2 + HO_2 \quad \text{(R8)}$$

$$OH + CH_4 + O_2 \rightarrow CH_3O_2 + H_2O \quad \text{(R9)}$$

$$OH + RH + O_2 \rightarrow RO_2 + H_2O \quad \text{(R10)}$$

$$HCHO + h\nu + 2O_2 \rightarrow 2HO_2 + CO \quad \text{(R11)}$$

$$HCHO + OH + O_2 \rightarrow HO_2 + CO + H_2O \quad \text{(R12)}$$

Perhydroxyl radicals (HO_2) or organic peroxyl radicals (RO_2) convert NO to NO_2, and are converted back to hydroxyl radicals (OH). Figure 8 gives an illustration of these relationships. Most importantly, the isoprene emissions can create a shift in the HO_x

cycle. Excessive amounts of isoprene can deplete OH radicals, producing HO_2 or RO_2 through Reaction (R13). Subsequently, under a NO_x-limited and isoprene-abundant environment, HO_2 and RO_2 radicals are removed from the atmosphere producing two products, hydrogen peroxides (H_2O_2) and organic hydroperoxides (ROOH), through Reactions (R15) and (R16), respectively.

$$OH + Isoprene(C_5H_8) \rightarrow RO_2 \text{ (multi-steps)} \quad \text{(R13)}$$

$$OH + Monoterpene(C_{10}H_{16}) \rightarrow RO_2 \text{ (multi-steps)} \quad \text{(R14)}$$

$$HO_2 + HO_2 \rightarrow H_2O_2 \quad \text{(R15)}$$

$$RO_2 + HO_2 \rightarrow ROOH \quad \text{(R16)}$$

Therefore, in summer, the modeled OH concentrations at the surface in China are quite low, due to the active conversion of OH to HO_2 and RO_2 by the presence of abundant isoprene (see the second column in Fig. 7). Therefore, if too large biogenic isoprene emissions are used in CMAQ modeling, the modeled (or virtual) NO_x levels could be higher than the actual NO_x levels. Indeed, the CMAQ-predicted NO_x chemical loss rates were slow during summer in the CMAQ modeling, as shown in Fig. 7. In contrast, the GOME-derived NO_2 columns during summer appear to be lower as a result of more active actual chemical destruction rates than virtual destruction rates. Such slow NO_x chemical loss rates resulted in higher NO_2 levels in the CMAQ modeling. In addition to isoprene, monoterpenes also convert OH to RO_2 via Reaction (R14). However, the CMAQ "v4.3" model only considered the gas-phase isoprene chemistry. The "MONO-TERP" species in the version of CMAQ 4.3 model did not take into account the gas-phase chemistry of monoterpenes, but considered secondary organic aerosol (SOAs) formation for monoterpenes (CMAS, 2003, 2006). The formation of SOAs from monoterpenes in East Asia was reported by Song et al. (2008). If gas-phase monoterpene chemistry is introduced in CMAQ modeling, the NO_x chemical loss rates would become even slower.

As mentioned in Sect. 2.2, the GEIA emission inventory was used to consider the biogenic emissions in CMAQ modeling. In this inventory, an isoprene flux of 20.0 Tg yr^{-1} over East Asia was estimated. However, Steiner et al. (2002) estimated an isoprene flux of only 13.6 Tg yr^{-1} over East Asia, using the land-cover conditions derived from the AVHRR satellite. Furthermore, Fu et al. (2007) recently estimated an even lower isoprene flux of 10.8 Tg yr^{-1} over East Asia from an inversion analysis of the GOME-retrieved HCHO columns. Overall, the isoprene flux used in this study might be approximately 1.5 to 2 times larger than those reported by Steiner et al. (2002) and Fu et al. (2007). As indicated by previous discussions, the rates of NO_x loss during summer in the CMAQ model simulations were lower than expected, which was attributed mainly to the lower OH concentrations. This might be due to the possible use of overestimated isoprene emissions in the modeling study. The rates of NO_x loss would be faster if the recent isoprene emissions in East Asia estimated by Fu et al. (2007) were used. Therefore, this study again confirmed that the biogenic emissions of the GEIA inventory could be overestimated in East Asia. Figure 9 shows that the NO_x chemical loss rates were changed at 2 km. The hydroxyl radical (OH) concentrations increase with decreasing isoprene concentrations, with a corresponding gradual increase in NO_x chemical loss rates.

In addition, the use of overestimated biogenic isoprene emissions in the CMAQ modeling can affect the NO_2/NO_x ratios. It is generally believed that there is some confidence in the ability of CTMs to simulate the actual NO_2/NO_x ratios (Martin et al., 2003). The current analysis was also based on the assumption that the actual NO_2/NO_x ratios could be successfully simulated by CMAQ modeling (Note that the GOME platform only measures the NO_2 columns, not the NO_x columns). Therefore, the correct NO_2 fractions are critical in this analysis (Leue et al., 2001). The NO_2/NO ratios at a pseudo-steady state can be estimated by Eq. (6):

$$\frac{[NO_2]}{[NO]} = \frac{k\,[O_3] + k'\,[HO_2] + k''\,[CH_3O_2] + k'''\,[RO_2]}{J_1} \quad (6)$$

ACPD
8, 17297–17341, 2008

where J_1 is the NO_2 photolysis reaction constant (s^{-1}); and k, k', k'', and k''' (cm^3 $molecules^{-1}$ s^{-1}) are the atmospheric reactions constants for the NO-to-NO_2 conversion reactions through NO+O_3, NO+HO_2, NO+CH_3O_2, and NO+RO_2, respectively. The concentrations of HO_2 and RO_2 might also be overestimated if the biogenic isoprene levels are over-predicted using the overvalued isoprene emissions in the CMAQ modeling (see Reaction R13; also refer to Fig. 8). This can lead to high NO_2/NO ratios in Eq. (6), which may result in incorrectly high NO_2/NO_x ratios in the CMAQ modeling. Figure 10 shows the NO_2/NO_x ratios over East Asia for the four episodes. The ratios were higher in summer than in the other seasons. Note the NO_2/NO_x ratios in Regions A and C. In addition, the NO_2/NO_x ratios in Region C were quite high during summer, >0.88, which is probably due to the high isoprene flux. By this reasoning, the CMAQ-modeled NO_2 columns shown in Figs. 3 and 4 might overestimate the actual NO_2 columns, which can lead to a further over-prediction in the CMAQ-simulated NO_2 column shown in Fig. 3.

However, in the ACE-ASIA NO_x emission inventory, the NO_x emissions from microbiological activity in soil were not considered, as mentioned previously. According to a recent satellite observation-constrained top-down NO_x inventory study reported by Wang et al. (2007), soil NO_x emissions can sometimes account for up to 43% of combustion sources during the summer in China, depending on the application of fertilizers as well as seasonally variable temperatures and precipitation. Both the retarded NO_x chemical loss rates and highly biased NO_2/NO_x ratios can lead to an over-prediction in the CMAQ-simulated NO_2 columns, whereas a consideration of soil NO_x emissions over North China during the summer might offset the effects from the overestimated biogenic isoprene emission fluxes. Overall, the natural emission of biogenic isoprene and soil-derived NO_x during the warm seasons in East Asia is uncertain and requires further investigation.

ACPD
8, 17297–17341, 2008

3.3 Emission inventories in East Asia

3.3.1 NO_x emission inventories for South Korea

As discussed previously, it was found that the CMAQ-predicted NO_2 columns over South Korea (C) may be overestimated by 41.14% to 117.63% compared with the GOME-derived NO_2 columns. This finding can be confirmed with the emission fluxes recently released from the NIER for South Korea: CAPSS inventory. The CAPSS emission inventory for South Korea has been built up since 1999 as a part of the "Total Air Pollution Load Management System". The CAPSS was established following the SNAP 97 (Selected Nomenclature for Air Pollution), which was used as the CORINAIR (CORe INventory of AIR emission) emission inventory system of the EEA (European Environment Agency). The CAPSS is an 1 km×1 km-resolved, very detailed emission inventory that employs a hybrid approach (a combination of bottom-up and top-down approaches), including intensive surveys on large-scale point sources (such as power plants, smelting facilities, and chemical & petrochemical plants), mobile sources with different automobile categories and classes, area sources with regional fuel-type consumption statistics, and non-road mobile sources such as vessels, aviation, and construction equipment. In detail, the CAPSS has the following major 11 classification codes: i) electric generating utility (EGU) combustion, ii) non-electric generating utility (NEGU) combustion, iii) industrial combustion, iv) industrial processes, v) storage and transport, vi) solvent utilization, vii) on-road mobile, viii) non-road mobile, ix) waste treatment, x) biogenic, and xi) agriculture (Heo et al., 2002; also, refer to http://airemiss.nier.go.kr).

The NO_x emission fluxes of the CAPSS inventory was compared with those of two other inventories available for South Korea for 2001: ACE-ASIA and REAS. The NO_x emission fluxes of the REAS inventory were obtained from the official REAS emission web site (http://www.jamstec.go.jp/frcgc/research/p3/emission.htm). Figure 11 shows the annual distribution of the NO_x emissions of the CAPSS inventory for the year 2001, showing high emission fluxes in metro-city areas such as Seoul, Incheon and Busan

ACPD
8, 17297–17341, 2008

(refer to Fig. 1, regarding the locations of these cities). Table 2 shows the NO_x emission fluxes of the CAPSS, ACE-ASIA and REAS emission inventories. The comparison shows that the NO_x emission fluxes of the ACE-ASIA and REAS inventories were approximately double that of the CAPSS inventory over Seoul and Incheon, and were approximately 3 times larger over the Busan and Ulsan areas. This is in line with the conclusions drawn from a previous comparison study between the CMAQ-predicted and the GOME-derived NO_2 columns, i.e. the NO_x emission fluxes of the ACE-ASIA inventory over South Korea were overestimated by 41.1%–117.6%. In addition, sulfur dioxide (another important primary pollutant) emission of the CAPSS inventory has a similar inconsistency to those of the ACE-ASIA and REAS inventories. As shown in Fig. 12, the SO_2 emission fluxes of the ACE-ASIA and REAS inventories were also larger than those of the CAPSS inventory, particularly around metro-city areas. Table 3 shows that the SO_2 emission fluxes of the ACE-ASIA and REAS were even ~10 times larger over the Seoul and Incheon areas than those of the CAPSS inventory, and ~2 times larger over the Busan and Ulsan areas. Therefore, in order to correctly consider the emissions from South Korea (C), the NO_x emissions from the ACE-ASIA and REAS inventory should be replaced by the NO_x emissions of the CAPSS inventory.

3.3.2 NO_x emission inventories for China

There are several NO_x emission inventories in China available for 2001 including i) ACE-ASIA/TRACE-P inventory (Streets et al., 2003), ii) REAS (Ohara et al., 2007), iii) EDGAR (Emission Database for Global Atmospheric Research) (Olivier et al., 1999, 2002), and iv) GEIA. Here, the ACE-ASIA and REAS inventories were used for a comparison study of the NO_x emission fluxes from China.

As discussed previously, when the ACE-ASIA inventory was used, the CMAQ-predicted NO_2 columns over North China (A) were underestimated by 8.6%–56.9%, compared with the GOME-derived NO_2 columns. In order to confirm this, the three emission inventories for China were inter-compared: ACE-ASIA, REAS, and "date-back" ANL inventory. Here, the "date-back" ANL inventory was estimated based on

an emission inventory developed recently by Zhang et al. (2007) for 2006. The ANL inventory for 2006 is an "upgraded" and "updated" version of the ACE-ASIA emission inventory. The former ("upgraded") indicates that the ANL inventory was improved and methodologically evolved. The latter ("updated") means that the ANL inventory reflects the rapidly-growing NO_x emissions from China (Zhang et al., 2007). The ANL inventory for 2006 also accounted for new emission factors, technology renewal, and bottom-up approaches for various emission sources. Since the ANL inventory is only available for "2006", an attempt was made to "date-back" the ANL inventory to "2001" by retaining the "upgraded" components of the ANL inventory but dating-back the "updated" parts of the ANL inventory to 2001. For this work, the NO_x emission shapes of the ANL inventory were retained but the NO_x emissions over China were reduced using China's statistical data as well as the increase in energy and fossil fuel consumption (Zhang et al., 2007).

Figure 13 shows the annual distribution of the NO_x emission fluxes of ACE-ASIA, "date-back" ANL, and REAS inventories in the upper panels. The differences in the NO_x emission fluxes are shown in the bottom panels of Fig. 13. While the differences between the REAS and ACE-ASIA inventories (Fig. 13e) were relatively small, the differences between "date-back" ANL and ACE-ASIA inventories (Fig. 13d) and between the "date-back" ANL and REAS inventories (Fig. 13f) were relatively large. The NO_x emission fluxes of the ACE-ASIA inventory are smaller than those of the "date-back" ANL inventory over North China (A). This was confirmed by analyzing the NO_x emission fluxes of the ACE-ASIA, "date-back" ANL and REAS emission inventory in Table 4. The comparison shows that the NO_x emission fluxes of the "date-back" ANL inventory were ~10% larger than those of the ACE-ASIA and REAS inventory over North China (A), and were approximately 30% larger than that of the ACE-AISA inventory over South China (B). The total amount of NO_x emission fluxes over North China (A) were largest in the "date-back" ANL inventory and smallest in the REAS inventory. Overall, the NO_x emission fluxes of the ACE-ASIA and REAS inventories were probably underestimated over North China (A), as was reported by Ma et al. (2006) and Uno et al. (2007). It is

ACPD
8, 17297–17341, 2008

believed that although the NO_x emissions of the "date-back" ANL inventory may be the closest to the real situations for 2001, the NO_x emission fluxes of the "date-back" ANL inventory were still low based upon comparisons of the CMAQ-predicted and GOME-derived NO_2 columns, in which there was 8.6%–56.9% underestimation in NO_x emissions over North China. Again, the correct emission inventory is a critical input for examining the source-receptor relationships. The importance of using the correct NO_x emission fluxes from North China for 2001 ("reference year" of the new Korean environmental policy of the "Total Air Pollution Load Management System") to examine the impact of Chinese emissions (source) on South Korean (receptor) air quality cannot be overemphasized.

4 Summary and conclusions

This study reports on comprehensive comparisons between the CMAQ-predicted and GOME-derived NO_2 columns in order to determine the accuracy of the NO_x emission inventory over North China (A) and South Korea (C). Since both regions have a strong source-receptor relationship, an accurate knowledge of the emissions over both the regions is vital for understanding the contributions of North China emissions to South Korean air quality. When the ACE-ASIA emission inventory for 2001 was used, the CMAQ-predicted NO_2 columns were low by 8.6%–56.9% over North China (A) and by 41.1%–117.6% over South Korea (C) compared with the GOME-derived NO_2 columns. This was further confirmed partly by comparing several emission inventories. The ACE-ASIA and REAS emission inventories showed large uncertainties over North China (A) and South Korea (C). The NO_x emission fluxes of the ACE-ASIA inventory over South Korea and North China were overestimated by ~50% and underestimated by ~10%, respectively, compared with the CAPSS and "date-back" ANL inventories. Based on these analyses, the "date-back" ANL and CAPSS inventories appear to provide a better estimation of the real situation over North China (A) and South Korea (C), respectively, even though the NO_x emissions of the "date-back" ANL inventory is

still low. In this study, the HO_x-NO_x-isoprene photo-chemistry in East Asia was also examined because they are strongly coupled with the NO_x chemical loss rates in North China (A) and South Korea (C). In particular, the biogenic emissions of isoprene and monoterpenes are the key parameter to control OH radicals, whose concentrations sequentially control the NO_x concentrations through nitric acid and particulate nitrate formation. Recent studies reported on lower biogenic NMVOC emissions in East Asia, which would imply that with the current emission inventory, the results of CMAQ modeling may significantly retard the rates of NO_x loss in East Asia, hence increase the NO_x levels, particularly during summer. Therefore in future, biogenic emissions should also be corrected to model the NO_x concentrations more precisely during summer in East Asia.

The correct emission inventory is critical for examining source-receptor relationships. Using the corrected emission inventories for North China (A) and South Korea (C), a one year-long Models-3/CMAQ modeling over East Asia is currently underway to examine and quantify more accurately the influences of Chinese (source) emissions on the South Korean (receptor) air quality.

Acknowledgements. This study was funded mainly by the Korea Ministry of Environment as an Eco-technopia 21 project under grant 121-071-055, and was also supported by the Korea Science and Engineering Foundation (KOSEF) grant (MEST) (No. R17-2008-042-01001-0).

References

Arndt, R., Carmichael, G.. R., and Roorda, J. M.: Seasonal source-receptor relationships in Asia, Atmos. Environ., 32, 1397–1406, 1998.

Binkowski, F. S. and Roselle, S. J.: Models-3 Community Multi-scale Air Quality (CMAQ) model aerosol components: 1. model description, J. Geophys. Res., 108(D6), 4183, doi:10.1029/2001JD001409, 2003.

Boersma, K. F., Eskes, H. J., and Brinksma, E. J.: Error Analysis for Tropospheric NO_2 retrieval from space, J. Geophys. Res., 109, D04311, doi:10.1029/2003JD003962, 2004.

Burrows, J. P., Dehn, A., Himmelmann, S., Richter, A., Voigt, S., and Orphal, J.: Atmospheric remote-sensing reference data from GOME: Part 1. Temperature-dependent absorption cross-sections of NO_2 in the 231-794nm range, J. Quant. Spectrosc. Radiat., 60, 1025–1031, 1998.

Burrows, J. P., Richter, A., Dehn, A., Deters, B., Himmelmann. S., Voigt, S., and Orphal, J.: Atmospheric remote-sensing reference data from GOME: Part 2. Temperature-dependent absorption cross-sections of O_3 in the 231–794 nm range, J. Quant. Spectrosc. Radiat., 61, 509–517, 1999.

Byun, D. W. and Ching, J. K. S.: Science algorithms of the EPA models-3 Community Multiscale Air Quality (CMAQ) modeling system, EPA/600/R-99/030, US EPA, Research Triangle Park, USA.

Byun, D. W. and Schere, K. L.: Review of the governing equations, computational algorithm, and other components of the Models-3 Community Multi-scale Air Quality (CMAQ) Modeling system, Appl. Mech. Rev., 59(2), 51–77, 2006.

CAPSS (Clean Air Policy Support System): National Institute of Environmental Research (NIER), South Korea, 2001.

CMAS (Community Modeling and Analysis System): CAMQ v4.3 release note, UNC, 2003

CMAS (Community Modeling and Analysis System): Operational guidance for the Community Multiscale Air Quality (CMAQ) modeling system, UNC, 2006.

Chance, K.: Analysis of BrO measurements from the Global Ozone Monitoring Experiment, Geophys. Res. Lett., 3335–3338, 1998.

Colella, P. and Woodward. P. L.: The Piecewise Parabolic Method (PPM) for gas dynamical simulation, J. Comput. Phys., 54, 174–201, 1984.

Draxler, R. R.: HYSPLIT4 User's guide, NOAA Tech, Memo ERL ARL-230, 1999.

Fahey, K. M. and Pandis, S. N.: Size-resolved aqueous-phase atmospheric chemistry in a three-dimensional chemical transport model, J. Geophys. Res., 108(D22), 4690, doi:10.1029/2003JD003564, 2003.

Fu, T., Jacob, D. J., Palmer, P. I., Chance, K., Wang, Y. X., Barletta, B., Blake, D. R., Staton, J. C., and Pilling, M. J.: Space-based formaldehyde measurements as constrains on volatile organic compound emissions in east and south Asia and implications for ozone, J. Geophys. Res., 112, D06312, doi:10.1029/2006JD007853, 2007.

Gery, M. W., Whitten, G. Z., Killus, J. P., and Dodge, M. C.: A photochemical kinetics mechanism for urban and regional scale computer modeling. J. Geophys. Res., 94, 12 925–12 956,

1989.
Greenblatt, G. D., Orlando, J. J., Burkholder, J. B., and Ravishankara, A. R.: Absorption measurements of oxygen between 330 and 1140 nm, J. Geophys. Res., 95, 18 577–18 582, 1990.
He, Y., Uno, I., Wang, Z., Ohara, T., Sugimoto, N., Shimizu, A., Richter, A., and Burrow, J. P.: Variations of the increasing trend of tropospheric NO_2 over central east China during the past decade, Atmos. Envrion., 41, 4865–4876, 2007.
Heo, J. S., Lee, D. K., Hong, J. H., Seok, K. S., Lee, D. G., and Eom, Y. S.: A proposal on the new air emission source categories, J. KOSAE, 18(3), 231–245, 2002.
Kato, N. and Akimoto, H.: Anthropogenic emissions of SO_2 and NO_x in Asia: Emission inventories, Atmos. Environ., 41, S171–S191, 2007.
Koelemeijer, R. B. A., Stammes, P., Hovenier, J. W., and de Haan, J. F.: A fast method for retrieval of cloud parameters using oxygen A band measurements from the Global Ozone Monitoring Instrument, J. Geophys. Res., 106(D4), 3475–3490, 2001.
Korean Ministry of Environment: Execution of special measurements to improve metropolitan atmospheric Environment, Korea Environmental Policy Bulletin, vol. IV, 2006.
Kunhikrishnan, T., Lawrence, M. G., von Kuhlmann, R., Richter, A., Ladstätter-Weißenmayer, A., and Burrows, J. P.: Analysis of tropospheric NO_x over Asia using the model of atmospheric transport and chemistry (MATCH-MPIC) and GOME-satellite observations, Atmos. Environ., 38, 581–596, 2004.
Leue, C., Wenig, M., Wagner, T., Klimm, O. Platt, U., and Jähne, B.: Quantitative analysis of NO_x emissions from global Ozone Monitoring Experiment satellite mage sequences, J. Geophys. Res., 106(D6), 5493–5505, 2001.
Ma, J., Richter, A., Burrow, J. P., Nüß, H., and van Aardenne, J. A.: Comparison of simulated tropospheric NO_2 over China with GOME satellite data, Atmos. Environ., 40, 593–604, 2006.
Martin, R. V., Jacob, D. J., Chance, K., Kurosu, T. P., Palmer, P. I., and Evans, M. J.: Global inventory of nitrogen oxide emissions constrained by space-based observation of NO_2 columns, J. Geophys. Res., 108(D17), 4537, doi:10.1029/2003JD003453, 2003.
Ohara, T., Akimoto, H., Kurokawa, J., Horii, N., Yamaji, K., Yan, X., and Hayasaka, T.: An Asian emission inventory of anthropogenic emission sources for the period 1980–2020, Atmos. Chem. Phys., 7, 4419–4444, 2007, http://www.atmos-chem-phys.net/7/4419/2007/.
Olivier, J. G. P., Bloos, J. P. J., Berdowski, J. J. M., Visschedijk, A. J. H., and Bouwman, A. F.:

A 1990 global emission invenotry of anthropogenic sources of carbon monoxide on 1°×1° developed in the framework of EDGAR/GEIA, Chemosphere, Global Change Sci., 1, 1–17, 1999.

Olivier, J. G. J., Peters, J. A. H. W., Bakker, J., Berdowski, J. J. M., Visschedijk, A. J. H., and Bloos, J. P. J.: Applications of EDGAR: emission database for global atmospheric research, Report on.: 410.200.051. RIVM, The Netherlands, 2002.

Pandis, S. N. and Seinfeld, J. H.: Sensitivity Analysis of a chemical mechanism for aqueous-phase atmospheric chemistry, J. Geophys. Res., 94(D1), 1105–1126, 1989.

Richter, A. and Burrows, J. P.: Retrieval of tropospheric NO_2 from GOME measurements, Adv. Space Res., 29, 16 673–16 683, 2002.

Richter, A., Burrows, J. P., Nüß, H., Granier, C., and Niemeier, U.: Increase in tropospheric nitrogen dioxide over China observed from space, Nature, 437, 129–132, 2005.

Rothman, L. S., Gamache, R. R.; Tipping, R. H., Rinsland, C. P., Smith, M. A. H., Benner, D. C., Devi, V. M., Flaud, J. M., Camy-Peyret, C., Perrin, A., Goldman, A., Massie, S. T., Brown, L. R., and Toth. R. A.: The HITRAN molecular database: editions of 1991 and 1992, J. Quant. Spectrosc. Radiat. Trans., 48, 469–507, 1992.

Rozanov, V., Diebel, D., Spurr, R. J. D., and Burrows, J. P.: GOMETRAN: A radiative transfer model for the satellite project GOME – the plane parallel version, J. Geophys. Res., 102, 16 683–16 695, 1997.

Schwartz, S. E.: Mass transport considerations pertinent to aqueous-phase reactions of gases in liquid-water clouds, Chemistry of Multiphase Atmospheric System, edited by: Jaeschke, W., Springer-Verlag, Berlin, 415–471, 1986.

Song, C. H., Park, M. E., Ahn, H. J., Lee, K. H., Lee, Y. J., Kim, J. Y., Han, K. M., Kim, J., Ghim, Y. S., and Kim, Y. J.: An investigation into seasonal and regional aerosol characteristics in East Asia using model-predicted and remotely-sensed aerosol properties, Atmos. Chem. Phys. Disscuss., 8, 8661–8713, 2008.

Stauffer, D. R. and Seaman, N. L.: Use of four-dimensional data assimilation in a limited-area mesoscale model. Part I: experiments with synoptic-scale data, Mon. Weather Rev., 118(6), 1250–1277, 1990.

Stauffer, D. L. and Seaman, N. L.: Multiscale four-dimensional data assimilation, J. Appl. Meteorol., 33(3), 416–434, 1994.

Steiner, A., Luo, C., Huang, Y., and Chameides, W. L.: Past and present-day biogenic volatile organic compound emissions in East Asia, Atmos. Environ., 36, 4895–4905, 2002.

Streets, D. G., Bond, T. C., Carmichael, G.. R., Fernandes, S. D., Fu, Q, He, D., Klimont, Z., Nelson, S. M., Tsai, N. Y, Wang. M. Q., Woo, J.-H., and Yarber, K. F.: An inventory of gaseous and primary aerosol emissions in Asia in the year 2000, J. Geophys. Res., 108(D21), 8809, doi:10.1029/2002JD003093, 2003.

Uno, I., He, Y., Ohara, T., Yamaji, K., Kurokawa, J.-I., Katayama, M., Wang, Z., Noguchi, K., Hayashida, S., Richter, A., and Burrows, J. P.: Systematic analysis of interannual and seasonal variations of model-simulated tropospheric NO_2 in Asia and comparison with GOME-satellite data, Atmos. Chem. Phys., 7, 1671–1681, 2007, http://www.atmos-chem-phys.net/7/1671/2007/.

van der A, R. J., Peters, D. H. M. U., Eskes, H., Boersma, K. F., Van Roozendael, M., De Smedt, I., and Kelder, H. M.: Detection of the trend and seasoanl variation in tropospheric NO_2 over China, J. Geophys. Res., 111, D12317, doi:10.1029/2005JD006594, 2006.

Vountas, M., Rozanov, V., and Burrows, J.: Ring effect: Impact of rotational Raman scattering on radiative transfer in earth's atmosphere, J. Quant. Spectrosc. Radiat. Trans., 60, 943–961, 1998.

Wang, Y., McElroy, M. B., Martic, R. V., Streets, D. G., Zhang, Q., and Fu, T. M.: Seasonal variability of NO_x emissions over east China constrained by satellite observations: Implications for combustion and microbial suources, J. Geophys. Res., 112, D06301, doi:10.1029/2006JD007538, 2007.

Wesely, M. L.: Parameterization of surface resistances to gaseous dry deposition inregional-scale numerical models, Atmos. Environ., 23, 1293–1304, 1989.

Zhang, Q., Streets, D. G., He, K., Wang, Y., Richter, A., Burrows, J. P., Uno, I., Jang, C. J., Chen, D., Yao, Z., and Lei, Y.: NO_x emission trends for China, 1995–2004: The view from the ground and the view from space, J. Geophys. Res., 112, D22306, doi:10.1029/2007JD008684, 2007.

Table 1. Statistical analysis for the comparisons between the CMAQ-predicted and GOME-derived NO_2 columns over East Asia.

			RMSE[a]	MNGE[b]	MB[a]	MNB[b]
CMAQ vs. GOME	A	Spring	**8.17**	**52.27**	−1.27	**−8.59**
		Summer	**1.40**	**39.57**	0.05	**5.43**
		Fall	**35.67**	**58.42**	−5.03	**−56.90**
		Winter	**28.61**	**59.04**	−3.48	**−22.21**
	B	Spring	1.61	77.92	0.43	61.34
		Summer	2.47	42.00	0.06	22.02
		Fall	3.21	31.03	−0.64	−10.36
		Winter[c]	–	–	–	–
	C	Spring	**24.06**	**90.88**	3.26	**79.78**
		Summer	**18.35**	**121.21**	2.95	**117.63**
		Fall	**38.75**	**54.47**	3.32	**41.14**
		Winter	**35.92**	**70.49**	4.30	**65.57**
	D	Spring	4.45	111.92	0.84	94.78
		Summer	3.90	81.00	0.87	55.51
		Fall	6.29	46.62	−0.58	−7.83
		Winter	4.46	74.76	0.29	32.79

A: North China; B: South China: C: South Korea: D: Japan

[a] Unit, $\times 10^{15}$ molecules cm^{-2}

[b] Unit, %

[c] Due to missing values

Table 2. Comparison of NO_x emissions among the CAPSS, REAS, and ACE-ASIA inventories over South Korea for 2001.

Region	ACE-ASIA[a]	REAS[a]	CAPSS[a]	ACE-ASIA/CAPSS	REAS/CAPSS
Seoul	232 059	328 256	135 771	1.71	2.42
Incheon	399 787	378 100	176 379	2.27	2.14
Busan and Ulsan	361 520	496 088	129 188	2.80	3.84
Daegu	115 438	106 483	103 422	1.12	1.03
Other region	249 236	332 832	375 032	0.66	0.89
Total	1 358 040	1 641 758	919 792	1.48	1.78

[a] Ton yr^{-1}

Table 3. Comparison of SO_2 emissions among the CAPSS, REAS, and ACE-ASIA inventories over South Korea for 2001.

Region	ACE-ASIA[a]	REAS[a]	CAPSS[a]	ACE-ASIA/CAPSS	REAS/CAPSS
Seoul	169 054	300 418	22 846	7.40	13.15
Incheon	309 937	268 019	34 093	9.90	7.86
Busan and Ulsan	174 177	194 050	92 894	1.88	2.09
Daegu	68 811	55 048	23 902	2.88	2.30
Other region	134 453	227 625	147 937	0.91	1.54
Total	856 433	1 045 159	321 673	2.66	3.25

[a] Ton yr^{-1}

ACPD
8, 17297–17341, 2008

Table 4. Comparisons of NO_x emission among ACE-ASIA, "date-back" ANL, and REAS inventories over China for 2001.

Region	ACE-ASIA[a]	"date-back" ANL[a]	REAS[a]	"Date-back" ANL/ACE-ASIA	REAS/ ACE-ASIA
North China (A)	6 063 087	6 586 730	5 995 179	1.09	0.99
South China (B)	2 145 335	2 726 533	2 609 364	1.27	1.22
Other region	2 790 983	3 521 353	2 889 506	1.26	1.04
Total	10 999 405	12 834 616	11 494 050	1.17	1.04

[a] Ton yr^{-1}

ACPD
8, 17297–17341, 2008

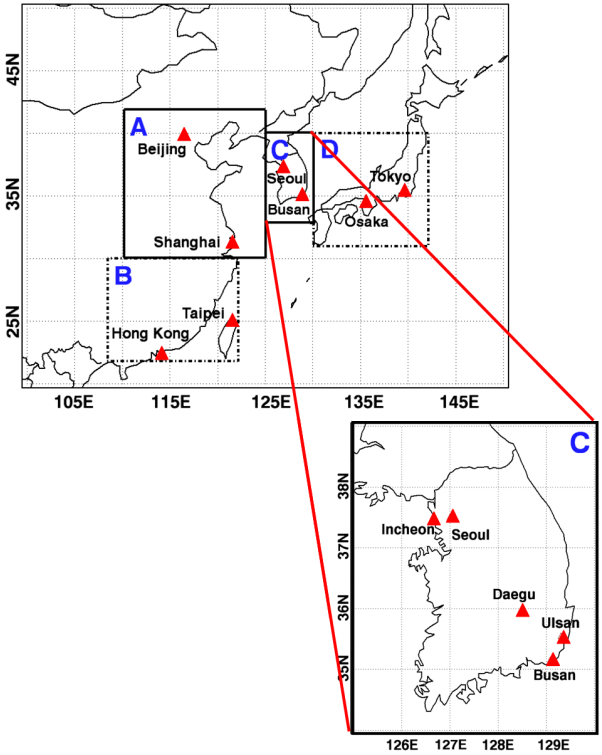

Fig. 1. Modeling domain of the study. Four regions were defined: i) A: North China, ii) B: South China, iii) C: South Korea, and iv) D: Japan.

ACPD

8, 17297–17341, 2008

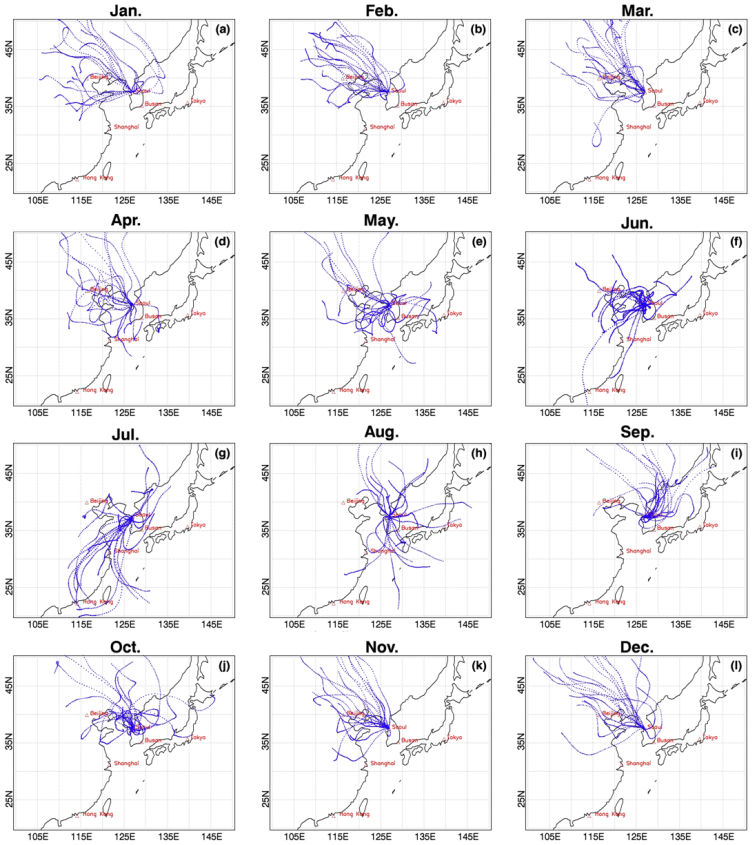

Fig. 2. Three-day backward trajectory analysis for air masses arriving in Seoul, Korea in 2001. The trajectories are obtained at 1 km a.s.l., and are shown at 1 h intervals: **(a)** January, **(b)** February, **(c)** March, **(d)** April, **(e)** May, **(f)** June, **(g)** July, **(h)** August, **(i)** September, **(j)** October, **(k)** November, and **(l)** December.

ACPD
8, 17297–17341, 2008

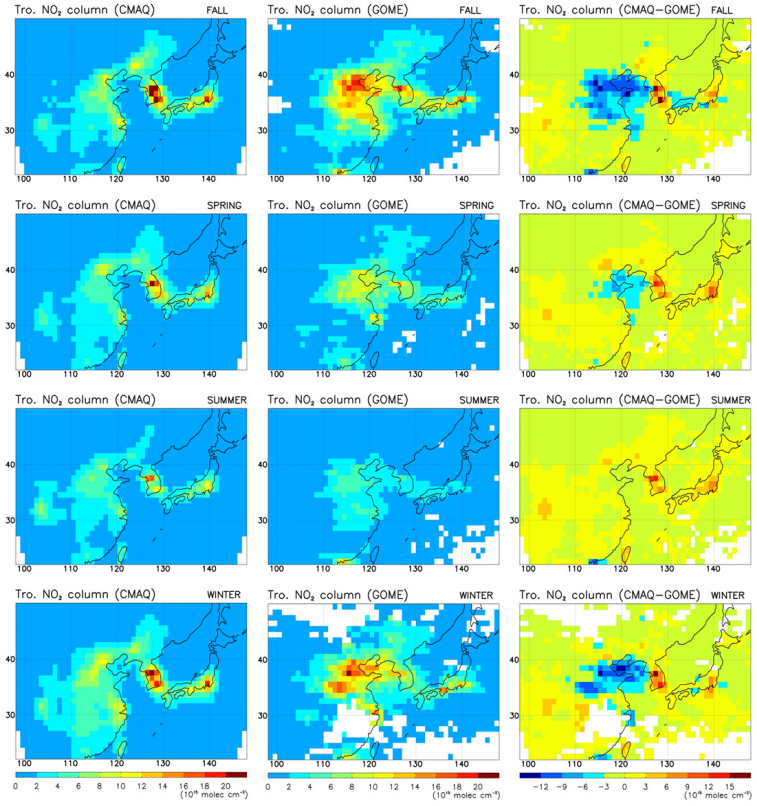

Fig. 3. Seasonal variations in the CMAQ-derived NO_2 columns (unit: $\times 10^{15}$ molecules cm^{-2}) in the first column and GOME-derived NO_2 columns in the second column (unit: $\times 10^{15}$ molecules cm^{-2}). The differences between the CMAQ-derived and GOME-derived NO_2 columns are shown in the third column.

ACPD
8, 17297–17341, 2008

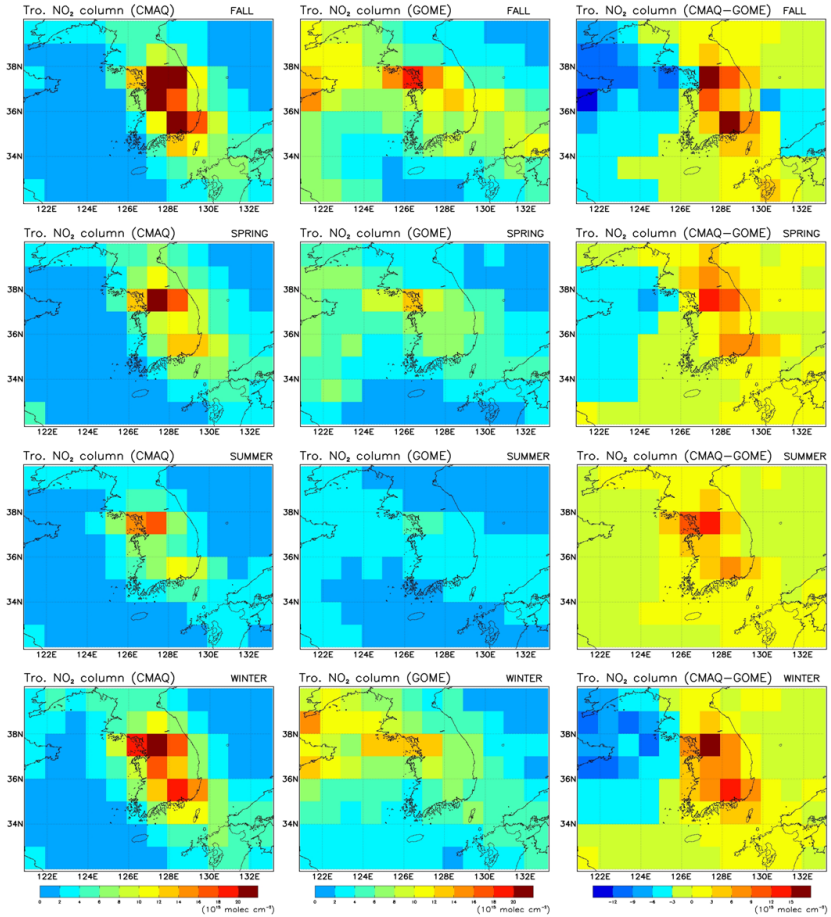

Fig. 4. As Fig. 3, except for closing in South Korea.

ACPD

8, 17297–17341, 2008

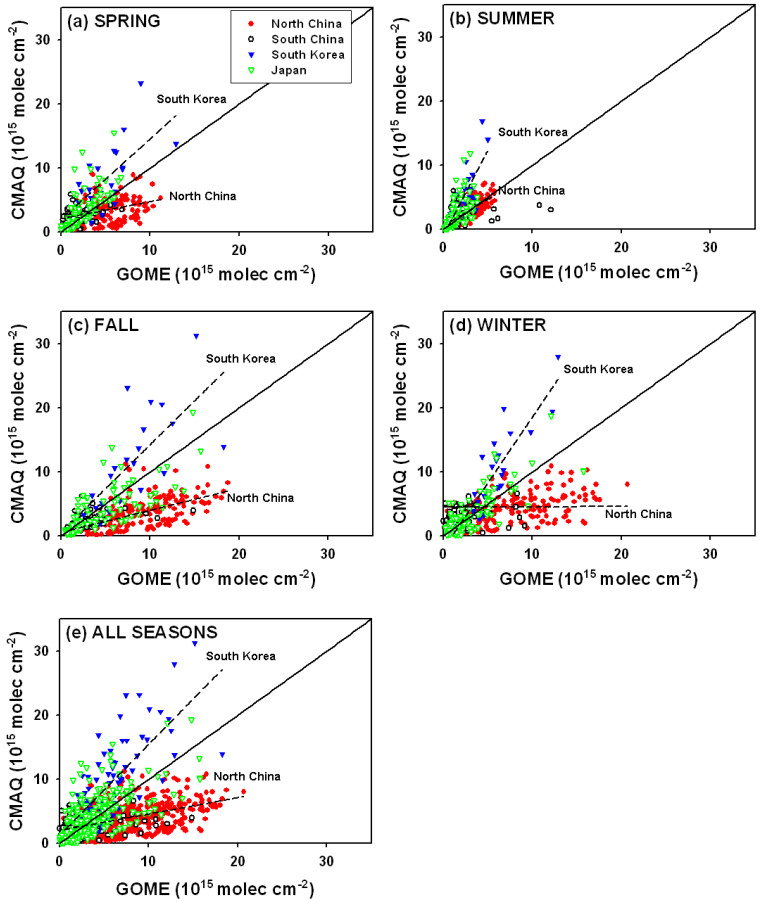

Fig. 5. Scatter plots between the CMAQ-derived and GOEM-derived NO_2 columns for **(a)** spring, **(b)** summer, **(c)** fall, **(d)** winter, and **(e)** all seasons. North China (red circles), South China (open circles), South Korea (blue triangles), and Japan (green triangles).

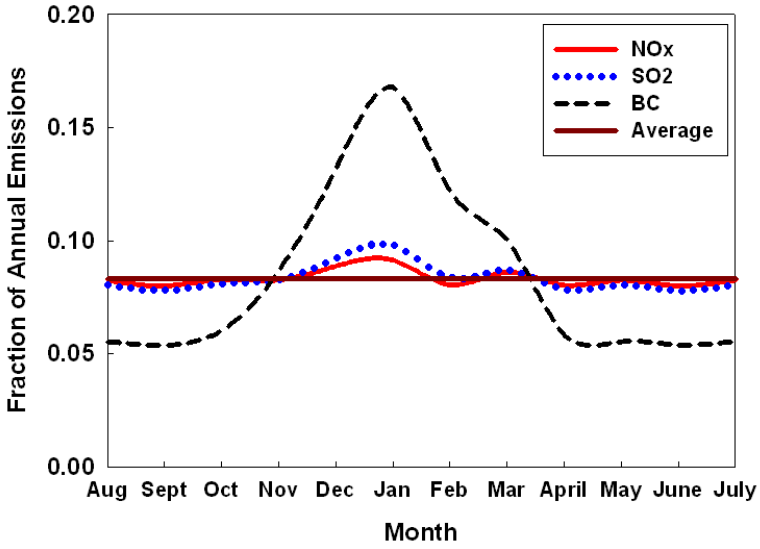

Fig. 6. Seasonal variations in the anthropogenic NO_x (red thick line), SO_2 (blue dot line), and BC (black dash line) emissions in China (Streets et al., 2003).

ACPD
8, 17297–17341, 2008

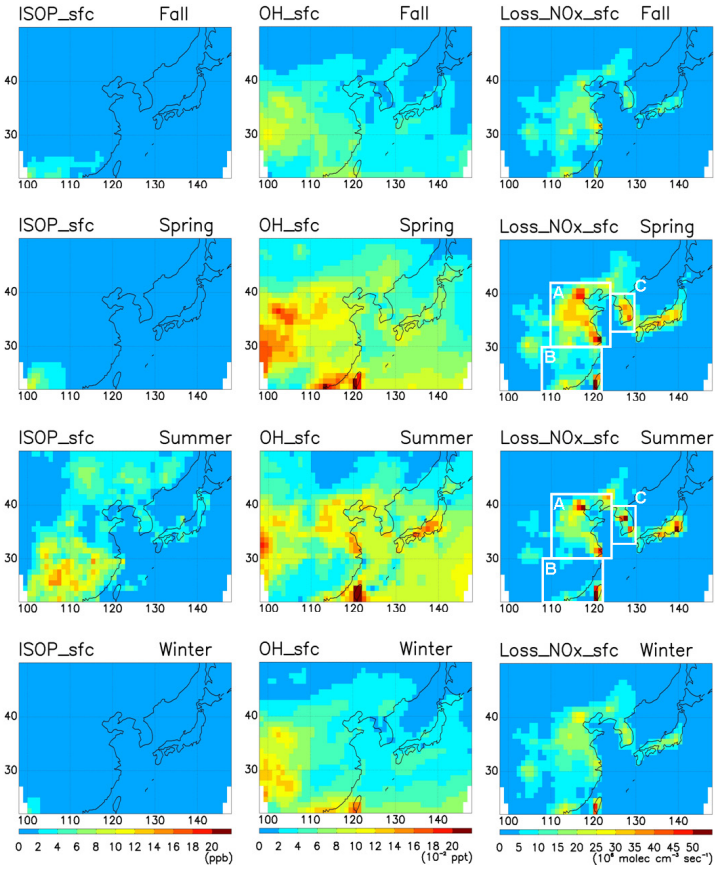

Fig. 7. Seasonal variations in the CMAQ-derived isoprene concentration (unit: ×ppb) at the surface level (the first column), CMAQ-derived hydroxyl radical (OH) concentration (unit: $\times 10^{-2}$ ppt) at the surface level (the second column), and NO_x loss rates (unit: $\times 10^{6}$ molecules cm^{-3} s^{-1}) at the surface level (the third column).

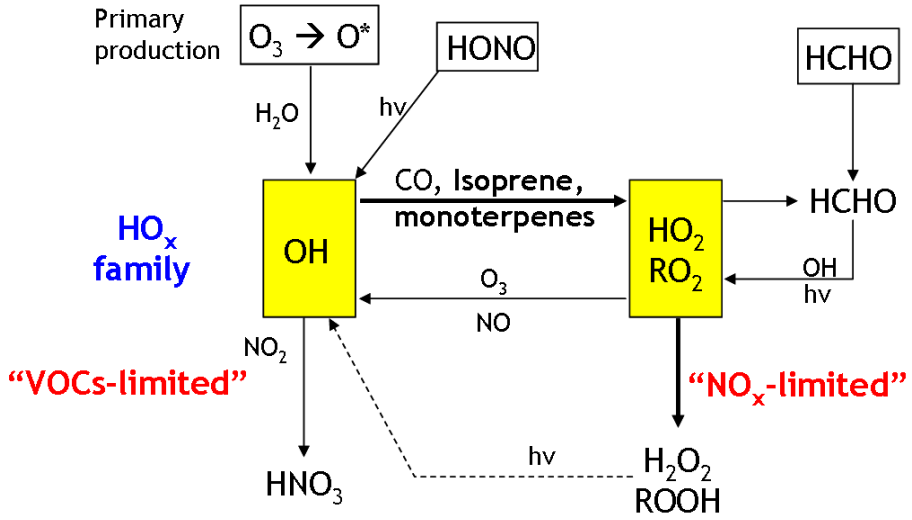

Fig. 8. An illustration of the simplified HO_x/RO_2-NO_x-biogenic VOC photochemistry.

ACPD
8, 17297–17341, 2008

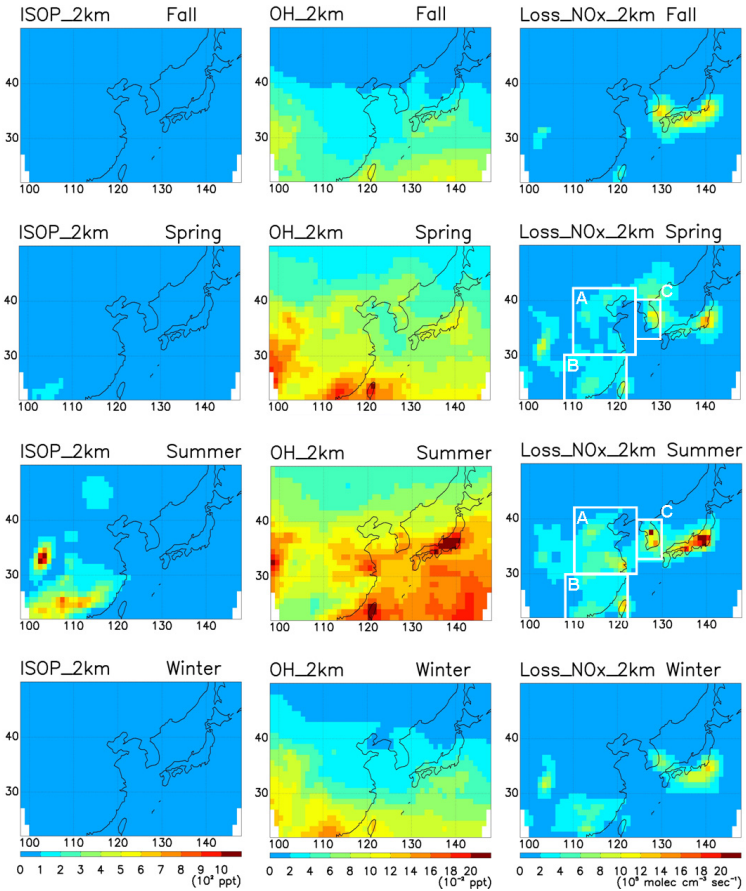

Fig. 9. Similar to Fig. 7, except for the isoprene concentrations (unit: $\times 10^2$ ppt), OH concentrations (unit: $\times 10^{-2}$ ppt), and NO_x loss rates (unit: $\times 10^5$ molecules cm^{-3} s^{-1}) at the 2 km.

ACPD
8, 17297–17341, 2008

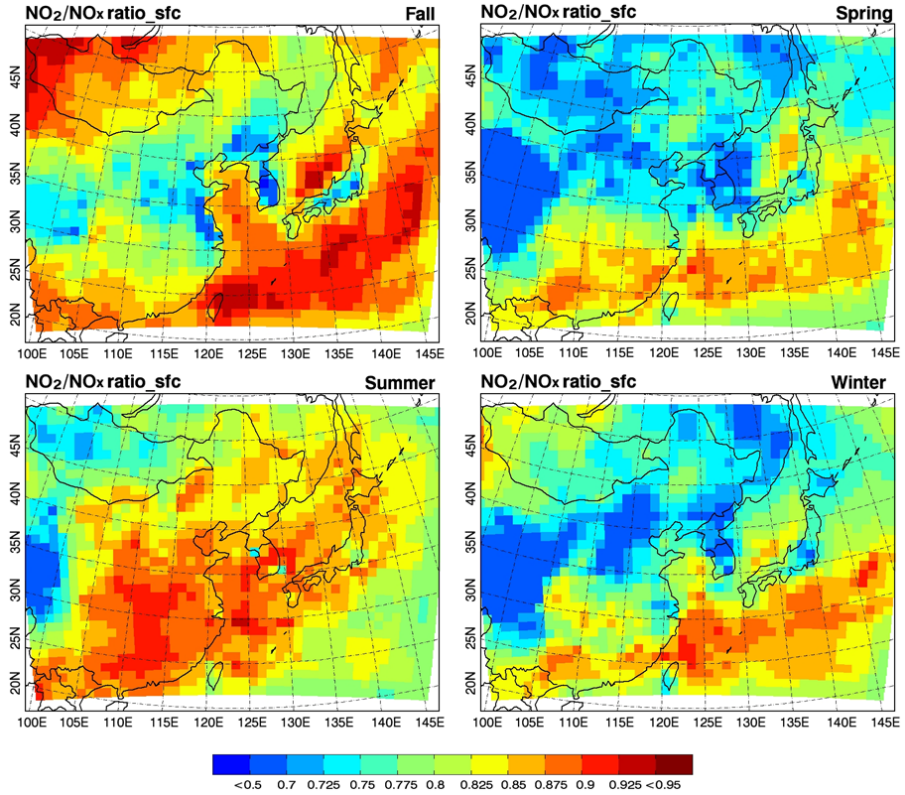

Fig. 10. NO_2/NO_x ratios modeled by CMAQ model: **(a)** Fall, **(b)** Spring, **(c)** Summer, and **(d)** Winter.

ACPD
8, 17297–17341, 2008

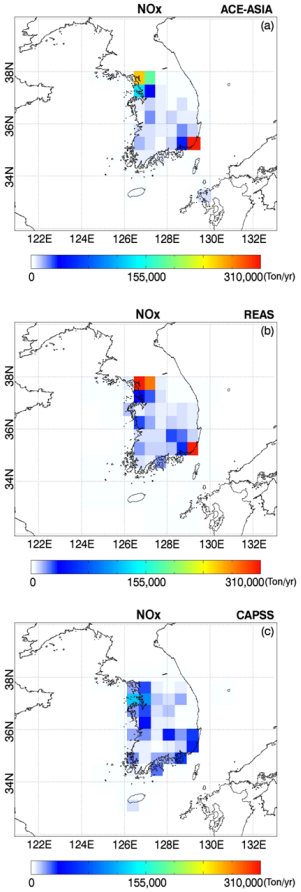

Fig. 11. Annual NO_x emission fluxes over South Korea: **(a)** ACE-ASIA, **(b)** REAS, and **(c)** CAPSS.

ACPD
8, 17297–17341, 2008

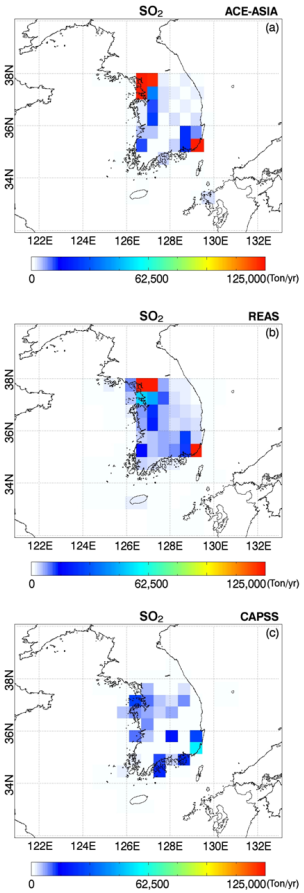

Fig. 12. Similar to Fig. 10, except for SO_2.

ACPD
8, 17297–17341, 2008

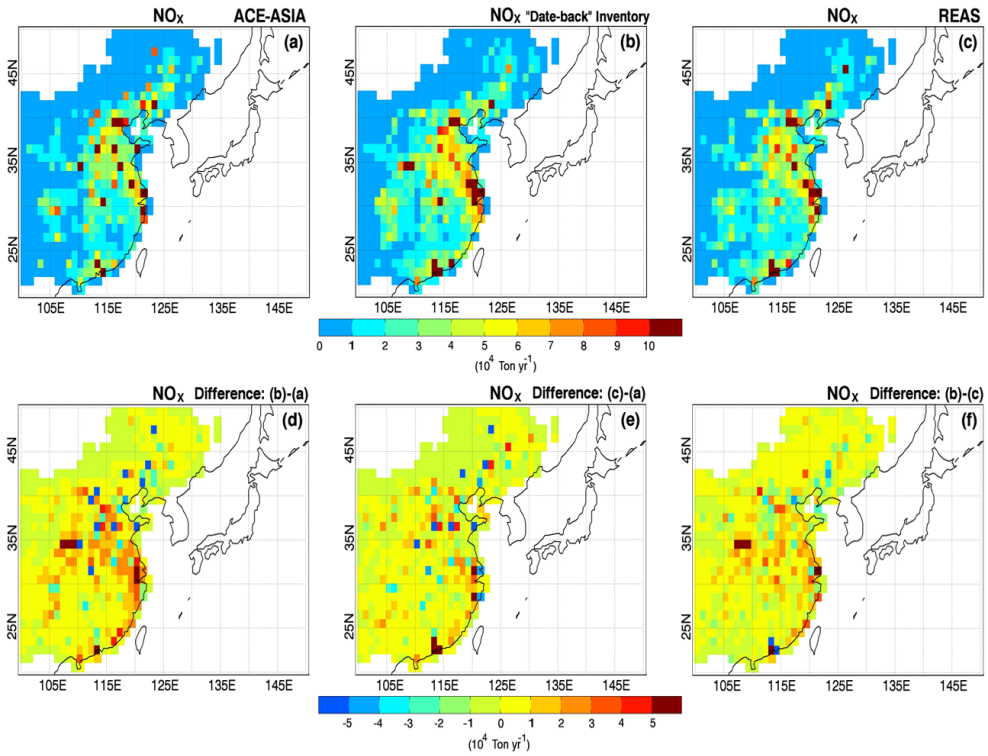

Fig. 13. Annual NO_x emissions inventory over China: **(a)** ACE-ASIA, **(b)** "date-back" ANL, and **(c)** REAS. The differences between the annual NO_x emission inventories are also shown in: **(d)** "date-back" ANL – ACE-ASIA, **(e)** REAS – ACE-ASIA, and **(f)** "date-back" ANL – REAS.

ACPD
8, 17297–17341, 2008